

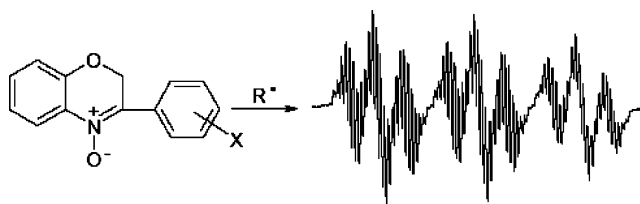
## Radical Trapping Properties of 3-Aryl-2H-benzo[1,4]oxazin-4-oxides

Paola Astolfi, Milvia Marini, and Pierluigi Stipa\*

Dipartimento di Scienze e Tecnologie Chimiche, Università Politecnica delle Marche, via Brecce Bianche, I-60131 Ancona, Italy

p.stipa@univpm.it

Received June 8, 2007



A series of 3-aryl-2H-benzo[1,4]oxazin-4-oxides was prepared, and their ability to trap free radicals was investigated by EPR spectroscopy. In organic solvents, these compounds were able to efficiently scavenge all carbon- and oxygen-centered radicals tested, giving very persistent aminoxyls, except with superoxide anion whose spin adducts were unstable. The main feature of these nitrones as spin traps lies in the possibility to recognize the initial radical trapped. In fact, besides a  $g$ -factor and aminoxyl nitrogen EPR coupling constant dependence on the species trapped, the EPR spectra also show different patterns due to hyperfine splittings characteristic of the radical scavenged. This last important feature was investigated by means of density functional theory calculations.

### Introduction

Electron paramagnetic resonance (EPR) spin trapping represents one of the most specific and reliable techniques for detecting and identifying transient free radicals, such as those produced in chemical and biological processes whose lifetime is too short in the EPR spectroscopic time scale. This technique, widely used since its introduction about 40 years ago,<sup>1</sup> is based upon the fast reaction between a suitable diamagnetic molecule (a spin trap) and short-lived free radicals with formation of relatively long-lived radicals (spin adducts), whose EPR signals are persistent enough to be recorded and analyzed: hyperfine coupling constants (hfccs) and  $g$ -factors are characteristic of the type of initial radical trapped.

Nitrones ( $N$ -oxides) are very efficient spin traps<sup>2</sup> being able to undergo fast radical additions with all kinds of radicals, C-centered and O-centered ones, to yield aminoxyls (nitroxides) as spin adducts, the most persistent organic free radicals in liquid solutions. Among all the commercially available nitrones,  $N$ -tert-butylbenzylideneamine  $N$ -oxide (PBN) and 5,5-dimethyl-3,4-

dihydro-2H-pyrrole  $N$ -oxide (DMPO) are the most popular, but their use is not without limitations. For example, PBN and its analogues give spin adducts with similar EPR spectra generally consisting of a triplet of doublets with a relatively small variation in the doublet splitting depending on the radical trapped, and this may be a source of misinterpretations in spin trapping experiments.<sup>3</sup> On the other hand, the use of DMPO is limited by its sensitivity to nucleophilic attack by water and the relatively low stability of its superoxide spin adduct which decomposes rapidly.<sup>4</sup> A continuous effort has been devoted to the synthesis of PBN and DMPO analogues<sup>5</sup> and of other nitrones<sup>6</sup> to be used in spin trapping experiments without the drawbacks associated with the above-mentioned common nitrones. To this end, we synthesized a series of 3-aryl-2H-benzo[1,4]oxazin-4-oxide derivatives and evaluated their spin trapping

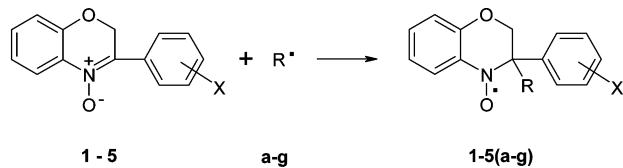
\* To whom correspondence should be addressed. Telephone and Fax: +39 071 2204409.

(1) (a) Mackor, A.; Wajer, Th. A. J. W.; de Boer, Th. J. *Tetrahedron Lett.* **1966**, 2115. (b) Iwamura, M.; Inamoto, N. *Bull. Chem. Soc. Jpn.* **1967**, *40*, 702. (c) Chalfont, G. R.; Perkins, M. J.; Horsfield, A. *J. Am. Chem. Soc.* **1968**, *90*, 7141. (d) Janzen, E. G.; Blackburn, B. J. *J. Am. Chem. Soc.* **1968**, *90*, 5909. (e) Lagerscrantz, C.; Forshult, S. *Nature* **1968**, *218*, 1247.

(2) (a) Janzen, E. G. *Acc. Chem. Res.* **1971**, *4*, 31. (b) Evans, C. A. *Aldrichimica Acta* **1979**, *12*, 23. (c) Mottley, C.; Mason, R. P. In *Biological Magnetic Resonance* 8; Berliner, L. J., Reuben, J., Eds.; Plenum Publishers: New York, 1989; p 489. (d) Tordo, P. *Electron Paramagn. Reson.* **1998**, *16*, 116. (e) Buettner, G. R. *Free Radical Biol. Med.* **1987**, *3*, 259. (f) Janzen, E. G.; Liu, J. I.-P. *J. Magn. Reson.* **1973**, *9*, 510. (g) Janzen, E. G.; Evans, C. A.; Liu, J. I.-P. *J. Magn. Reson.* **1973**, *9*, 513. (h) Janzen, E. G. In *Free Radicals in Biology*; Prior, W. A., Ed.; Academic Press: New York, 1980; p 115.

(3) Kotake, Y.; Janzen, E. G. *J. Am. Chem. Soc.* **1991**, *113*, 9503.

(4) (a) Makino, K.; Hagiwara, T.; Imaishi, H.; Nishi, M.; Fuji, S.; Ohya, H.; Murakami, A. *Free Radical Res. Commun.* **1990**, *9*, 233. (b) Finkelstein, E.; Rosen, G. M.; Rauckman, E. J. *Mol. Pharmacol.* **1982**, *21*, 262.

**SCHEME 1. Formation of Spin Adducts 1–5(a–g) from Nitrones 1–5**


- |                             |                                |
|-----------------------------|--------------------------------|
| 1 : X = H                   | a : R = OH                     |
| 2 : X = Cl                  | b : R = OO                     |
| 3 : X = 2'-OCH <sub>3</sub> | c : R = OO <sup>-</sup> tBu    |
| 4 : X = 3'-OCH <sub>3</sub> | d : R = CH <sub>3</sub>        |
| 5 : X = 4'-OCH <sub>3</sub> | e : R = Ph                     |
|                             | f : R = CH <sub>2</sub> -Ph    |
|                             | g : R = C(Me <sub>2</sub> )-CN |

ability by EPR spectroscopy. Two structural features of these compounds which could both have a stabilizing effect on the corresponding spin adducts prompted us to test these nitrones as potential spin traps: the absence of  $\alpha$ -hydrogens to the nitrene function and the presence of an oxygen atom on the benzoxazinic ring. In fact, it is known that aminoxyls bearing  $\alpha$ -hydrogens are unstable and may disproportionate to the corresponding nitrene and a hydroxylamine,<sup>7</sup> and it has been observed that electron-withdrawing substituents close to the N–O function<sup>5e,8</sup> could stabilize spin adducts, in particular, those deriving from superoxide trapping. Density functional theory (DFT) calculations were also performed, exploiting the recent developments in the area<sup>9</sup> which led to computational methods able to describe the properties of free radicals, including their EPR features, with an excellent level of confidence.<sup>10</sup>

**Results and Discussion**

The studied derivatives are listed in Scheme 1 together with the corresponding spin adducts. All nitrones tested have been known since 1979,<sup>11</sup> but their ability to trap free radicals had never been checked.

As a representative view of the geometry of these compounds, the ball and stick molecular geometry of **1** computed at the B3LYP/6-31G(d) level, together with the corresponding highest

occupied molecular orbital (HOMO) plot, is reported in Figure 1; the arbitrary atom labeling used in Figure 1 is maintained throughout the whole text.

These calculations gave N(13)–C(14) and N(13)–O(15) bond distances of  $1.332 \pm 0.002$  and  $1.280 \pm 0.002$  Å, respectively, for all nitrones, in good agreement with the literature reports.<sup>12</sup> It was found that the N(13)–C(14) double bond is almost coplanar with the aromatic ring of the benzoxazine moiety (out-of-plane angle of about 12°) and that an excellent coplanarity with the above-mentioned ring exists also for O(10). A dihedral angle of 179° is formed between O(10), C(1), C(3), and C(5) which allows delocalization of the nonbonding electrons, as shown by the HOMO plot (Figure 1b). On the other hand, C(12) lies out of that plane at about 28°, and protons H(16) and H(17), magnetically equivalent in the corresponding <sup>1</sup>H NMR spectra, become diastereotopic after radical addition. The aromatic ring present at C(14) is only slightly twisted (about 18°) with respect to the virtual benzoxazine plane, except for derivative **3**. In this latter nitrone, the presence of the –OCH<sub>3</sub> substituent at the 2' position of the phenyl ring produces a significant increase in the corresponding N(13)–C(14)–C(18)–C(20) dihedral angle, resulting in an enhanced steric hindrance which could justify the selective reactivity found for this nitrone toward some of the tested radicals, such as superoxide and 2-cyano-2-propyl. The bond distances and dihedral angles computed for all nitrones that were selected for comparison purposes are reported in Table 1.

Spin trapping ability of nitrones **1–5** was tested by generating the radicals directly in the EPR tube containing a benzene degassed solution of the nitrone under study. In particular, a Fenton reaction system (FeSO<sub>4</sub>/H<sub>2</sub>O<sub>2</sub>) was used for producing OH• radicals (in this case, the solvent was 5% H<sub>2</sub>O in [1,4]-dioxane instead of benzene), whereas KO<sub>2</sub> in the presence of a crown ether was used as a source of superoxide radical anion (OO•<sup>-</sup>). *tert*-Butylperoxyls as well as methyl, phenyl, and benzyl radicals were generated by in situ lead dioxide oxidation of *tert*-butylhydroperoxide, methyl, phenyl, and benzyl magnesium bromide reagents, respectively, while 2-cyano-2-propyl radicals were obtained from the thermal decomposition of 2,2'-azobisisobutyronitrile (AIBN). Nitrones **1–5** are all able to trap both carbon- and oxygen-centered radicals, giving persistent aminoxyls as spin adducts whose EPR spectra (Figure 2) remain unchanged for hours in argon-deaerated solutions. The kinetic decay of these spin adducts has not been studied yet, and at present, a comparison between the stability of these adducts and those obtained with the conventional traps (DMPO, PBN, and their analogues) still has to be done. However, particularly evident is the stability (rather than the persistency) of the spin adducts obtained in this work from trapping C-centered radicals. In fact, in most of the cases, it is possible to isolate and characterize the corresponding aminoxyls.<sup>13</sup> As for trapping O-centered radicals, it is noteworthy that spin adducts obtained from OH• and *t*-BuOO• are persistent aminoxyls, whereas OO•<sup>-</sup> is rapidly trapped by all the nitrones, but the spin adducts are unstable and rapidly decompose, making the acquisition of the

(5) (a) Hinton, R. D.; Janzen, E. G. *J. Org. Chem.* **1992**, *57*, 2646. (b) Zeghdaoui, A.; Tuccio, B.; Finet, J.-P.; Cerri, V.; Tordo, P. *J. Chem. Soc., Perkin Trans. 1* **1995**, 2087. (c) Janzen, E. G.; Zhang, Y.-K.; Haire, D. L. *Magn. Reson. Chem.* **1994**, *32*, 711. (d) Fréjaville, C.; Karoui, H.; Tuccio, B.; Le Moigne, F.; Culcasi, M.; Pietri, S.; Lauricella R.; Tordo, P. *J. Chem. Soc., Chem. Commun.* **1994**, 1793. (e) Fréjaville, C.; Karoui, H.; Tuccio, B.; Le Moigne, F.; Culcasi, M.; Pietri, S.; Lauricella R.; Tordo, P. *J. Med. Chem.* **1995**, *38*, 258. (f) Stolze, K.; Udilova N.; Nohl, H. *Biol. Chem.* **2002**, *383*, 813. (g) Stolze, K.; Udilova, N.; Rosenau, T.; Hofinger A.; Nohl, H. *Biol. Chem.* **2003**, *384*, 493. (h) Zhao, H.; Joseph, J.; Zhang, H.; Karoui H.; Kalyanaraman, B. *Free Radical Biol. Med.* **2001**, *31*, 599. (i) Olive, G.; Mercier, A.; Le Moigne, F.; Rockenbauer A.; Tordo, P. *Free Radical Biol. Med.* **2000**, *28*, 403.

(6) (a) Tsai, P.; Pou, S.; Straus, R.; Rosen, G. M., *J. Chem. Soc., Perkin Trans. 2* **1999**, 1759. (b) Rosen, G. M.; Tsai, P.; Barth, E. D.; Dorey, G.; Casara, P.; Spedding, M.; Halpern, H. J. *J. Org. Chem.* **2000**, *65*, 4460.

(7) (a) Dupeyre, R.-M.; Rassat, A. *J. Am. Chem. Soc.* **1966**, *88*, 3180. (b) Adamic, K.; Bowman, D. F.; Gillan, T.; Ingold, K. U. *J. Am. Chem. Soc.* **1971**, *93*, 902.

(8) (a) Karoui, H.; Nsanzumuhire, C.; Le Moigne, F.; Tordo, P. *J. Org. Chem.* **1999**, *64*, 1471. (b) Allouch, A.; Roubaud, V.; Lauricella, R.; Bouteiller, J.-C.; Tuccio, B. *Org. Biomol. Chem.* **2005**, *3*, 2458.

(9) (a) Parr, R. G.; Yang, W. In *Density Functional Theory of Atoms and Molecules*; Oxford University Press: New York, 1998. (b) Koch, W.; Holthausen, M. C. *A Chemist's Guide to Density Functional Theory*; Wiley-VCH: Weinheim, Germany, 2000.

(10) For a review, see: Improta, R.; Barone, V. *Chem. Rev.* **2004**, *104*, 1231.

(11) Battistoni, P.; Bruni, P.; Fava, G. *Tetrahedron* **1979**, *35*, 1771.

(12) (a) Villamena, F. A.; Hadad, C. M.; Zweier, J. L. *J. Am. Chem. Soc.* **2004**, *126*, 1816. (b) Villamena, F.; Dickman, M. H.; Crist, D. R. *Inorg. Chem.* **1998**, *37*, 1446. (c) Boeyens, J. C. A.; Kruger, G. J. *Acta Crystallogr.* **1970**, *B26*, 668. (d) Xu, Y. K.; Chen, Z. W.; Sun, J.; Liu, K.; Chen, W.; Shi, W.; Wang, H. M.; Zhang, X. K.; Liu, Y. *J. Org. Chem.* **2002**, *67*, 7624.

(13) Astolfi, P.; Stipa, P. Unpublished results.

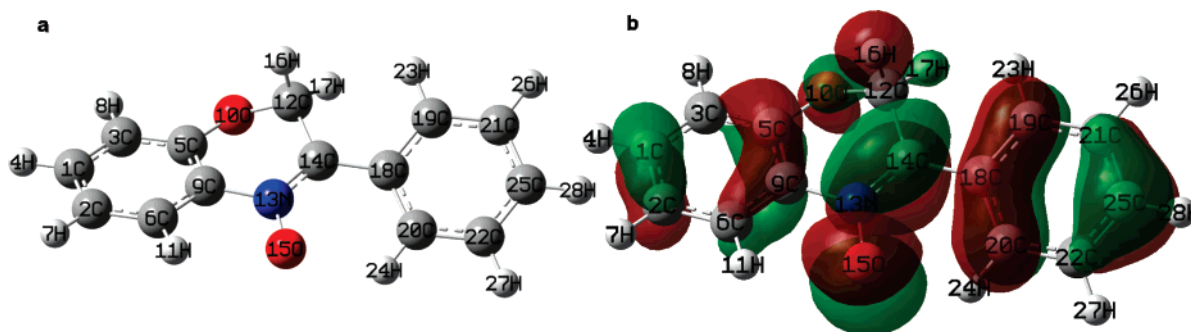


**FIGURE 1.** “Ball and stick” optimized geometry computed at the B3LYP/6-31G(d) level (a) and HOMO plot (b) computed at the B3LYP/6-31+G(d,p) level of nitrone **1** showing the arbitrary atom labeling.

**TABLE 1.** Selected Bond Distances (angstroms), Dihedral Angles (degrees), and Dipole Moment ( $\mu$ /Debye) for Nitrones **1–5** Computed at the B3LYP/6-31+G(d,p)// B3LYP/6-31G(d) Level; Partition Coefficients ( $K_p$ ) Refer to 1-Octanol/Phosphate Buffer at pH 7.4

	N(13)–C(14)	N(13)–O(15)	C(1)–C(3)–C(5)–O(10)	C(3)–C(5)–O(10)–C(12)	C(6)–C(9)–N(13)–C(14)	N(13)–C(14)–C(18)–C(20)	$\mu$	$K_p$
1	1.33	1.28	179.22	27.58	11.36	18.45	2.569	12.25
2	1.33	1.28	179.20	27.66	11.35	17.27	3.544	8.32
3	1.33	1.28	179.47	28.87	12.40	34.41	3.985	8.44
4	1.33	1.28	179.29	27.56	11.32	18.96	2.555	10.81
5	1.33	1.28	179.19	27.52	11.10	17.16	4.057	1.08

corresponding EPR spectra particularly difficult as in the case of adduct **3b** whose spectrum was not recorded.

A subset of nitroxides “experimental” hfccs obtained by means of spectral simulation are collected in Table 2. The complete listing of all hfccs together with the correlation coefficient between experimental and simulated spectra and the mean absolute deviation<sup>14</sup> (MAD) can be found in Table S1 in Supporting Information. A good agreement between the calculated coupling constants and the experimental ones was found, but when superoxide trapping was possible, only the replacement of  $\text{OO}^{\bullet-}$  with  $\text{HOO}^{\bullet}$  in the corresponding DFT calculations gave hfccs values in satisfactory agreement with the experimental results. This implies that protonation could in some way occur in the reaction medium as suggested for the corresponding DMPO analogue.<sup>15</sup> The relatively low correlation coefficient between experimental and simulated spectra reported in Table S1 for aminoxyls **1–5c** could be likely due to the superimposition of different signals. It is known, in fact, that  $t\text{-BuOO}^{\bullet}$  radicals can undergo self-reaction, forming the corresponding tetraoxide which then decomposes giving molecular oxygen and  $t\text{-BuO}^{\bullet}$  radicals.<sup>16</sup> These last can, in turn, undergo  $\beta$ -scission, yielding methyl radicals and acetone:<sup>17</sup> all radicals eventually formed in the reaction medium could be trapped by nitrones **1–5**, and their EPR signal could contribute, with different extent, to the final spectrum observed. Moreover, where adducts **1–5a** are concerned, similar EPR signals, although less resolved, have been obtained with the Fenton reaction system, replacing dioxane with pyridine as solvent, confirming that, in these cases, an intervention of C-centered radicals arising from hydrogen abstraction by  $\text{HO}^{\bullet}$  on dioxane could be likely excluded. Finally, the assignment of the HO proton coupling in **1–5a** has been carried out by means of the isotopic exchange technique; as a

typical example, in Figure S1 in Supporting Information, the experimental EPR spectra sequence for adduct **1a**, together with their corresponding simulations, have been reported.

In all cases, complex EPR signals are obtained because of the coupling of the unpaired electron with the benzoxazine ring hydrogen atoms. However, each spectrum is specific for the particular trapped radical being characterized by well-defined hfccs and  $g$ -factors which vary according to the nature of the radical species. This represents one of the main favorable features of this class of nitrones which allows the unequivocal identification of a particular spin adduct and hence of the parent free radical, despite the absence of the additional hyperfine splitting due to the hydrogen atom at the  $\alpha$ -carbon<sup>2e–g</sup> which normally aids in the characterization of the trapped species. Moreover, from the analysis of the hfccs collected in Table 2, it is possible to highlight some trends in their values which well correlate with the nature of the trapped radical. For example, if H(17) hfccs for all spin adducts are considered, it is found that they always reach the highest value in aminoxyls **1–5c** derived from  $t\text{-BuOO}^{\bullet}$  trapping, likely due to a possible through space interaction between H(17) and O(30) of the peroxy group (as shown in Supporting Information Figure S2). On the other hand, H(16) hfccs are always smaller than H(17), likely for geometrical reasons, reaching maximum values in superoxide adducts. Other information on the nature of the particular radical trapped may be deduced from the full analysis of the corresponding EPR spectrum. An example is represented by EPR spectra of  $\text{Ph-CH}_2^{\bullet}$  adducts **1–5f**, all characterized by the splittings due to the diastereotopic benzylic protons, as already found in indolinonic aminoxyls.<sup>18</sup> To confirm these findings, DFT calculations were performed using the multistep procedure previously described,<sup>19</sup> and strong similarities with indolinonic aminoxyls were found. In Figure 3, the single occupied molecular orbital (SOMO) and the total spin density ( $\alpha-\beta$ )

(14) MAD: average difference between the computed and experimental values ignoring the sign: Foresman, J. B.; Frisch, A. *Exploring Chemistry with Electronic Structure Methods*; Gaussian Inc.: Pittsburgh, PA, 1996; p 145.

(15) Villamena, F. A.; Merle, J. K.; Hadad, C. M.; Zweier, J. L. *J. Phys. Chem. A* **2005**, *109*, 6083.

(16) Griller, D.; Ingold, K. U. *Acc. Chem. Res.* **1980**, *13*, 193.

(17) Batt, L.; Robinson, G. N. *Int. J. Chem. Kinet.* **1982**, *14*, 1053.

(18) Berti, C.; Colonna, M.; Greci, L.; Marchetti, L. *Tetrahedron* **1975**, *31*, 1745.

(19) Stipa, P. *Chem. Phys.* **2006**, *323*, 501.

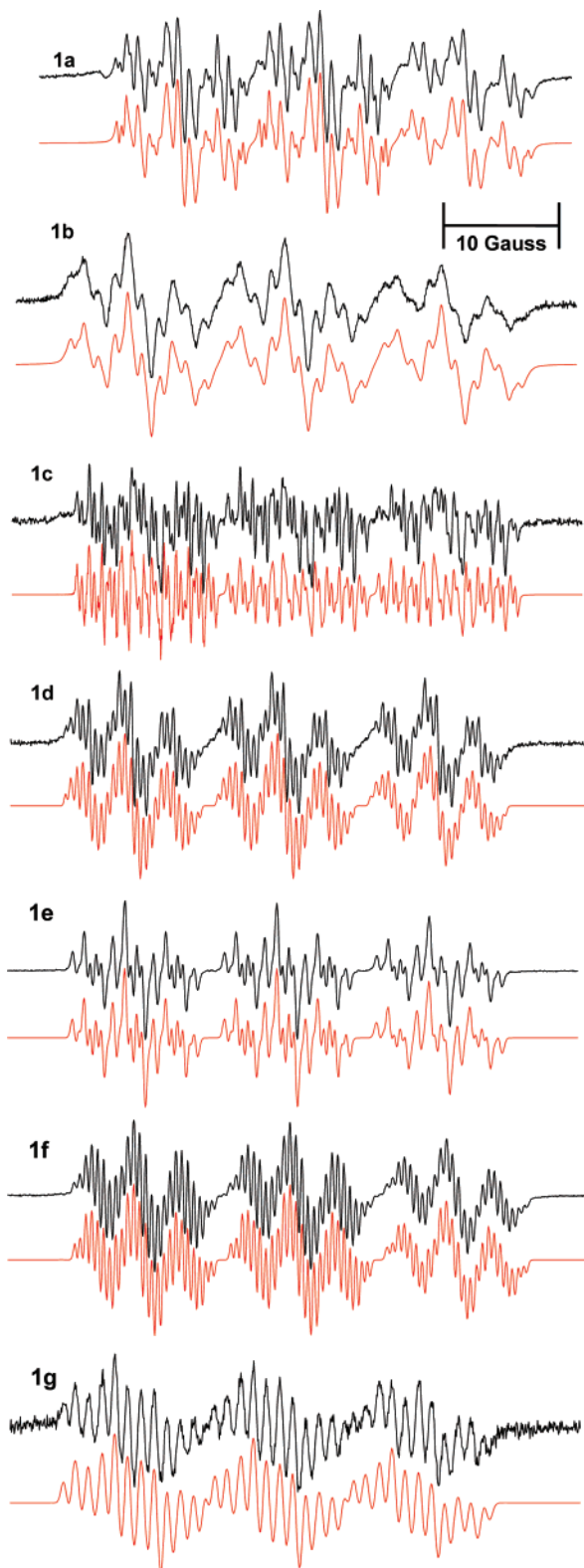


**FIGURE 2.** Experimental (black) and simulated (red) liquid solution EPR spectra of aminoxyls **1–5(a–g)** (magnetic field strength in Gauss); spectrometer settings are reported in the Experimental Section.

distribution plot of **1d** computed at the B3LYP/EPR-III level<sup>20</sup> are reported as an example.

(20) Barone, V. In *Recent Advances in Density Functional Methods*; Chong, D. P., Ed.; World Scientific Publ. Co.: Singapore, 1966; Part 1.

**TABLE 2.** Selected Hyperfine Coupling Constants (hfccs in Gauss) and *g*-Factors of Spin Adducts **1–5(a–g)** in Benzene Solutions in Accordance with the Arbitrary Atom Labeling of Figure 1

spin adduct	hfcc				<i>g</i>
	H-16	H-17	N-13	R <sup>b</sup>	
<b>1a<sup>a</sup></b>	0.34	0.74	10.71	−0.66	2.00560
<b>1b</b>	0.39	0.81	11.19	—	2.00548
<b>1c</b>	0.30	1.42	10.59	0.09 (3H)	2.00576
<b>1d</b>	0.32	0.71	10.64	0.50 (3H)	2.00558
<b>1e</b>	0.38	0.73	10.67	—	2.00566
<b>1f</b>	0.27	0.75	10.84	0.48; 0.39	2.00558
<b>1g</b>	0.30	0.62	9.73	0.92 (1N)	2.00579
<b>2a<sup>a</sup></b>	0.23	0.86	10.95	−0.61	2.00562
<b>2b</b>	0.31	0.67	10.93	—	2.00545
<b>2c</b>	0.28	1.46	10.59	0.09 (3H)	2.00574
<b>2d</b>	0.16	0.57	10.67	0.46 (3H)	2.00566
<b>2e</b>	0.35	0.73	10.70	—	2.00570
<b>2f</b>	0.27	0.79	10.86	0.46; 0.39	2.00558
<b>2g</b>	0.21	0.73	9.73	0.86 (1N)	2.00577
<b>3a<sup>a</sup></b>	0.43	0.83	10.71	−0.60	2.00563
<b>3d</b>	0.15	0.68	10.70	0.42 (3H)	2.00565
<b>3g</b>	0.22	0.68	9.72	0.86 (1N)	2.00571
<b>4a<sup>a</sup></b>	0.34	0.74	10.63	−0.72	2.00562
<b>4b</b>	0.51	0.81	11.25	—	2.00558
<b>4c</b>	0.30	1.44	10.62	0.09 (3H)	2.00554
<b>4f</b>	0.30	0.78	10.83	0.48; 0.41	2.00561
<b>4g</b>	0.22	0.73	9.77	0.84 (1N)	2.00579
<b>5a<sup>a</sup></b>	0.34	0.71	10.58	−0.70	2.00565
<b>5b</b>	0.51	0.81	11.31	—	2.00548
<b>5c</b>	0.28	1.47	10.62	0.09 (3H)	2.00549
<b>5d</b>	0.25	0.83	10.72	0.50 (3H)	2.00565
<b>5f</b>	0.27	0.76	10.89	0.49; 0.39	2.00558
<b>5g</b>	0.19	0.74	9.79	0.85 (1N)	2.00578

<sup>a</sup> Solvent 5% H<sub>2</sub>O in [1,4]dioxane. <sup>b</sup> When not specified, value(s) refer to proton(s) of the R group.

These pictures clearly show that the SOMO is extended over the whole benzoxazine system and that negative spin densities were found for H(4) and H(11), justifying the sign of the corresponding hfccs values, in agreement with what was previously observed in the indolinonic analogues.

As for N hyperfine coupling, it is worth recalling that spin density in aminoxyls is mainly located on the N–O• group<sup>21</sup> with typical values for alkyl aminoxyls of about 14–15 G, but if conjugation with an aromatic system is possible, the corresponding hfccs are somewhat smaller because spin delocalization occurs.<sup>22</sup> This is the case of N(13) hyperfine couplings determined for the aromatic aminoxyls obtained in the present work ranging from 9.72 (**3g**) to 11.31 G (**5b**) as well as for other aromatic aminoxyls described in the literature.<sup>18,19,22</sup> Moreover, N(13) hfccs may also be affected by the nature of the radical added to the α-carbon C(14) since this latter species may contribute both to the delocalization of the unpaired electron and to the geometry of the whole system. In particular, geometric factors such as bond distances and out of plane angles<sup>10</sup> could influence the value of nitrogen hyperfine coupling. Data reported in Table 2 indicate a variation in N(13) hfccs depending on the particular radical trapped, with the highest values for HOO• adducts and the lowest ones for 2-cyano-2-propyl radical (spin adducts **1–5g**). In this latter case, relatively large hfccs values (0.8–0.9 G) were found for the nitrogen atom of the cyano group which takes part in the delocalization of the unpaired electron. From the above discussion, it is clear that analysis of aminoxyl N-coupling could be a useful approach for the identification of the species trapped by these nitrones.

It is known that in organic free radicals the isotropic *g*-factor deviates from the corresponding value of the free electron

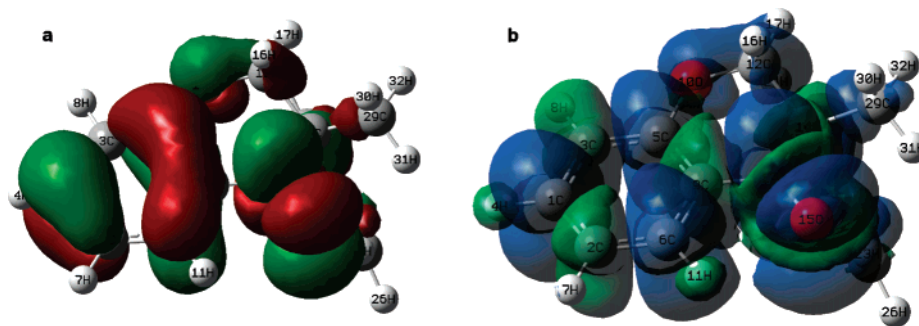


**FIGURE 3.** Single occupied molecular orbital (SOMO) (a) and  $\alpha$ - $\beta$  spin density distributions (b) of **1d** computed at the unrestricted B3LYP/EPR-III level. Positive spin densities are shown in red (a) and blue (b), while negative ones are always in green.

(2.0023) due to spin-orbit coupling effects arising from the contribution of each individual atom. As a consequence, the contribution of a specific group results from all its atoms and will be larger the more the odd electron is delocalized onto that group, producing the corresponding deviation of  $g$  from the free electron value. These substituent shifts of  $g$  in  $\pi$ -type radicals (including aminoxyls) are quite characteristic of the radical structure.<sup>23</sup> Analysis of the data collected in Table 2 reveals  $g$  changes with the trapped radical, the maximum values being usually found for **1-5g**, where the  $-\text{CN}$  group participates in the delocalization of the unpaired electron, while the minimum for **1-5b** spin adducts. This last finding represents another important feature of the studied nitrones because the  $g$ -value estimation of a spin adduct could possibly be used for the identification of the trapped radical together with N(13) hfccs and with the specific pattern of the EPR spectrum. A plot of N(13) hfccs versus  $g$ -factor values for **1a-g** confirms the relationship experimentally found between aminoxyl nitrogen coupling and  $g$ -value for each radical trapped (Figure 4).

Taking into account the increasing number of spin trapping applications in biological milieu,<sup>24</sup> the use of these nitrones is subjected to their solubility in aqueous and/or lipid systems, as quantified by 1-octanol/water partition coefficient. In fact, if the transient free radicals are produced in an aqueous environment, more hydrophilic nitrones could work better than hydrophobic ones. On the other hand, lipophilic nitrones are required

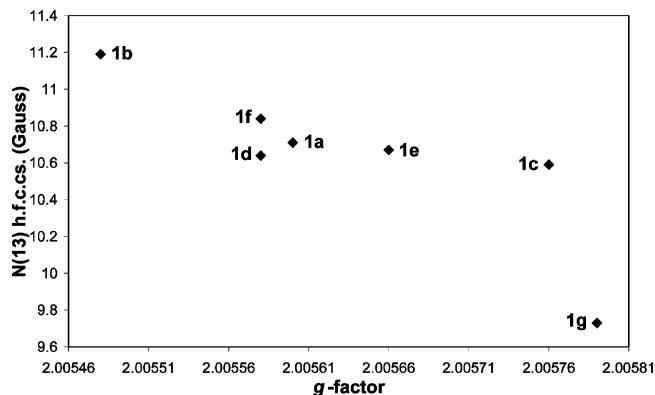


**FIGURE 4.** N(13) hfccs versus  $g$ -factor plot for adducts **1a-g**.

when the spin trapping technique is used in the detection of free radicals derived from lipid peroxidation.<sup>25</sup> These goals can be achieved through the design of spin traps whose differential solubility could allow the detection of free radicals in different tissue compartments and, eventually, in biomembranes. Hence the availability of a range of spin traps with different lipophilicity/hydrophilicity is welcome.

DFT calculations suggest that the introduction of groups such as  $-\text{Cl}$  or  $-\text{OCH}_3$  in different positions of the phenyl at C(14) of compound **1** can result in a sensitive increase in the corresponding nitron dipole moment ( $\mu$ , Table 1). These expectations were confirmed by the 1-octanol/phosphate buffer (pH 7.4) partition coefficient ( $K_P$ ) determined for all studied nitrones (see Table 1). The obtained values range from 12.5 of derivative **1**, the most lipophilic of the series whose  $K_P$  is comparable to that of PBN,<sup>26</sup> to 1.08 of nitron **5**, the most hydrophilic one, with a  $K_P$  comparable to those of BMPO<sup>27</sup> and DPPMPO,<sup>25</sup> although still far from the 0.09 value reported for DMPO.<sup>28</sup>

At present, our work is directed to the synthesis of more hydrophilic spin traps, possibly able to give more persistent adducts with superoxide anion and, at the same time, to the synthesis of nitrones yielding adducts with simpler EPR spectra, but still characteristic of the trapped radical.

(21) (a) Di Matteo, A.; Adamo, C.; Cossi, M.; Barone, V.; Rey, P. *Chem. Phys. Lett.* **1999**, *310*, 159. (b) Di Matteo, A.; Adamo, C.; Barone V.; Rey, P. *J. Phys. Chem.* **1999**, *103*, 3481. (c) Di Matteo, A.; Bencini, A.; Cossi, M.; Barone, V.; Mattesini M.; Totti, F. *J. Am. Chem. Soc.* **1998**, *120*, 7069. (d) Barone, V.; Grand, A.; Luneau, D.; Rey, P.; Minichino, C.; Subra, R. *New J. Chem.* **1993**, *17*, 545. (e) Cirujeda, J.; Vidal-Gancedo, J.; Jürgens, O.; Mota, F.; Novoa, J. J.; Rovira C.; Veciana, J. *J. Am. Chem. Soc.* **2000**, *122*, 11393. (f) Zheludev, A.; Barone, V.; Bonnet, M.; Delley, B.; Grand, A.; Ressouche, E.; Rey, P.; Subra, R.; Schweizer, J. *J. Am. Chem. Soc.* **1994**, *116*, 2019. (g) Mattar, S. M.; Stephens, A. L. *Chem. Phys. Lett.* **2000**, *319*, 601.

(22) Beyer, M.; Fritscher, J.; Feresin, E.; Schiemann, O. *J. Org. Chem.* **2003**, *68*, 2209.

(23) Fischer, H. In *Free Radicals*; Kochi, J. K., Ed.; Wiley-Interscience: New York, 1973; Vol. II, p 435.

(24) (a) Pou, S.; Halpern, H. J.; Tsai, P.; Rosen, G. M. *Acc. Chem. Res.* **1999**, *32*, 155. (b) Halliwell B.; Gutteridge, J. M. C. *Free Radicals in Biology and Medicine*, 2nd ed.; Clarendon Press: Oxford, 1989. (c) Korthuis, D.; Carden, D. L.; Granger, D. N. In *Biological Consequences of Oxidative Stress*; Spatz, L.; Bloom, D., Eds.; Oxford Press: London, 1992; p 50. (d) Schulz, J. B.; Henshaw, D. R.; Siwek, D.; Jenkins, B. G.; Ferrante, R. J.; Cipolloni, P. B.; Kowall, N. W.; Rosen B. R.; Beal, M. F. *J. Neurochem.* **1995**, *64*, 2239. (e) Harbour, J. R.; Chow, V.; Bolton, J. R. *Can. J. Chem.* **1974**, *52*, 3549. (f) Finkelstein, E.; Rosen, G. M.; Rauckman, E. J.; Paxton, J. *Mol. Pharmacol.* **1979**, *16*, 676. (g) Kalyanaram, B.; Perez-Reyes, E.; Mason, R. P. *Biochim. Biophys. Acta* **1980**, *630*, 119.

(25) Stolze, K.; Udilova, N.; Nohl, H. *Free Radical Biol. Med.* **2000**, *29*, 1005.

(26) Koronev, E. A.; Baker, J. E.; Joseph, J.; Kalyanaram, B. *Free Radical Biol. Med.* **1993**, *14*, 127.

(27) Turner, M. J., III; Rosen, G. M. *J. Med. Chem.* **1986**, *29*, 2439.

(28) Rosen, G. M.; Finkelstein, E.; Rauckman, E. J. *Arch. Biochem. Biophys.* **1982**, *215*, 367.

## Conclusions

A series of 3-aryl-2*H*-benzo[1,4]oxazin-4-oxides was prepared and tested as spin traps by EPR spectroscopy. All nitrones tested were able to efficiently scavenge all carbon- and oxygen-centered radicals used in this study. Their 1-octanol/phosphate buffer at pH 7.4 partition coefficient ranges from 12.25 to 1.08, thus allowing a wide range of possible applications in biological systems. The resulting spin adducts, except those deriving from superoxide trapping, are represented by very persistent aminoxyls, whose EPR signals did not vary in time in argon-deaerated benzene solutions. The dependence of both *g*-factor and aminoxyl nitrogen hfccs on the species trapped, together with the characteristic EPR splittings due to the radical trapped, could facilitate the identification of the radical itself, thus making the use of such scavengers more interesting. This important behavior is finally supported by suitable DFT calculations performed for all spin adducts.

## Experimental Section

All chemicals were of the highest grade of purity commercially available and used without further purification. IR spectra were recorded in Nujol on a spectrophotometer equipped with a Spectra Tech. "Collector" for DRIFT measurements. <sup>1</sup>H NMR and <sup>13</sup>C NMR spectra were recorded at room temperature in CDCl<sub>3</sub> at 199.975 and 50.289 MHz, respectively. Mass spectra were recorded in EI<sup>+</sup> mode. Isotropic X-band EPR spectra were recorded on a spectrometer system equipped with a microwave frequency counter and an NMR Gauss meter for field calibration; for *g*-factor determination, the whole system was standardized with a sample of perylene radical cation in concentrated sulfuric acid (*g* = 2.00258); general EPR spectrometer settings: microwave power 2 mW, modulation amplitude 0.2 G, time constant 0.64 ms, receiver gain 4.48 × 10<sup>4</sup>, sweep time 1342.177 s, conversion time 1310.720 ms; EPR spectrometer settings for transient adducts **1-5b**: microwave power 5 mW, modulation amplitude 0.2 G, time constant 0.080 ms, receiver gain 4.48 × 10<sup>4</sup>, sweep time 335.544 s, conversion time 327.680 ms. EPR spectra simulations were carried out by means of the Winsim program, freely available from NIEHS.<sup>29</sup>

Partition coefficients *K<sub>p</sub>* were determined at room temperature by means of UV spectrophotometry from the difference in absorbance at a fixed  $\lambda$  of freshly prepared solutions (0.15 mM) of nitrones in 1-octanol, before and after mixing with equal volumes of 5 mM pH 7.4 phosphate buffer, followed by 1 h vigorously stirring and separation by centrifugation (5000*r* for 2 min).

(29) Duling, D. *PEST Winsim*, version 0.96; National Institute of Environmental Health Sciences: Triangle Park, NC, 1996.

(30) Frisch, M. J.; Trucks, G. W.; Schlegel, H. B.; Scuseria, G. E.; Robb, M. A.; Cheeseman, J. R.; Montgomery, J. A., Jr.; Vreven, T.; Kudin, K. N.; Burant, J. C.; Millam, J. M.; Iyengar, S. S.; Tomasi, J.; Barone, V.; Mennucci, B.; Cossi, M.; Scalmani, G.; Rega, N.; Petersson, G. A.; Nakatsuji, H.; Hada, M.; Ehara, M.; Toyota, K.; Fukuda, R.; Hasegawa, J.; Ishida, M.; Nakajima, T.; Honda, Y.; Kitao, O.; Nakai, H.; Klene, M.; Li, X.; Knox, J. E.; Hratchian, H. P.; Cross, J. B.; Bakken, V.; Adamo, C.; Jaramillo, J.; Gomperts, R.; Stratmann, R. E.; Yazyev, O.; Austin, A. J.; Cammi, R.; Pomelli, C.; Ochterski, J. W.; Ayala, P. Y.; Morokuma, K.; Voth, G. A.; Salvador, P.; Dannenberg, J. J.; Zakrzewski, V. G.; Dapprich, S.; Daniels, A. D.; Strain, M. C.; Farkas, O.; Malick, D. K.; Rabuck, A. D.; Raghavachari, K.; Foresman, J. B.; Ortiz, J. V.; Cui, Q.; Baboul, A. G.; Clifford, S.; Cioslowski, J.; Stefanov, B. B.; Liu, G.; Liashenko, A.; Piskorz, P.; Komaromi, I.; Martin, R. L.; Fox, D. J.; Keith, T.; Al-Laham, M. A.; Peng, C. Y.; Nanayakkara, A.; Challacombe, M.; Gill, P. M. W.; Johnson, B.; Chen, W.; Wong, M. W.; Gonzalez, C.; Pople, J. A. *Gaussian 03*, revision D.02; Gaussian Inc.: Wallingford, CT, 2004.

DFT calculations were performed by means of the Gaussian 03 package<sup>30</sup> on an IBM SP5 supercomputer. All calculations on paramagnetic species were carried out with the unrestricted formalism, giving  $\langle S^2 \rangle = 0.7501 \pm 0.0001$  for spin contamination (after annihilation), and performed following the multistep procedure previously described;<sup>19</sup> in addition, in frequency calculations, imaginary (negative) values were never found, confirming that the computed geometries were always referred to a minimum.

**Synthesis of Benzoxazine Nitrones.** Nitrones **1-5** were prepared according to the literature reports:<sup>11</sup> in a typical run, the 2-nitrophenoxy acetophenone resulting from the alkaline condensation between 2-nitrophenol and the appropriate  $\alpha$ -bromoacetophenone underwent reductive cyclization (Zn/NH<sub>4</sub>Cl), affording the corresponding 3-aryl-2*H*-benzo[1,4]oxazin-4-oxide in low to moderate yield.

**Spin Trapping Studies.** Spin trapping experiments were performed by generating the radical to be trapped directly in the sample tube in the presence of the nitron under investigation in argon-deaerated benzene (0.1 mM) solutions. A different solvent, namely, [1,4]dioxane, was used in the trapping of HO<sup>•</sup> radicals.

The Fenton system was used to generate HO<sup>•</sup> radicals: aqueous FeSO<sub>4</sub> (10  $\mu$ M) was added to a [1,4]dioxane degassed solution of the nitron (0.1 mM) in the presence of 20  $\mu$ M hydrogen peroxide. EPR spectra were recorded 40 s after the addition of FeSO<sub>4</sub>.

A 10  $\mu$ M benzene solution of potassium superoxide KO<sub>2</sub> was used as source of superoxide anion prepared by adding the minimum amount of 18-crown-6 necessary to ensure complete solubility of KO<sub>2</sub> in benzene.

*tert*-Butylperoxyl radicals were generated by adding traces of solid lead dioxide (PbO<sub>2</sub>) to a degassed benzene solution containing 0.1 mM nitron and 10  $\mu$ M *tert*-butylhydroperoxide nonane solution. Methyl, phenyl, and benzyl radicals were produced by in situ PbO<sub>2</sub> oxidation of the corresponding Grignard reagent from commercial ethereal solutions as previously described.<sup>31</sup> 2-Cyano-2-propyl radicals were generated by thermal decomposition of 2,2'-azobisisobutyronitrile (AIBN), added as a solid to the starting nitron solution.

**Acknowledgment.** Università Politecnica delle Marche (Ancona, Italy) is kindly acknowledged for financial support and for providing a substantial amount of CPU time at Cineca Supercomputing Center (via Magnanelli 6/3, I-40033 Casalecchio di Reno, Bologna, Italy; <http://www.cineca.it/HPSsystems>).

**Supporting Information Available:** Hyperfine coupling constants (hfccs in Gauss), *g*-factors, correlation coefficient, and mean absolute deviation (MAD) of all spin adducts (Table S1); isotopic exchange experiment EPR spectra sequence for adduct **1a** (Figure S1); ball and stick optimized molecular geometry computed at the B3LYP/6-31G(d) level of aminoxyl **1c** (Figure S2); B3LYP/6-31+G(d,p)//B3LYP/6-31G(d) Cartesian coordinates and thermochemical parameters for all nitrones; B3LYP/6-31G optimized geometries Cartesian coordinates for all aminoxyls; 1-octanol solution UV spectra of nitrones **1-5** before and after mixing with equal volumes of pH 7.4 phosphate buffer for *K<sub>p</sub>* determination. This material is available free of charge via the Internet at <http://pubs.acs.org>.

JO071212I

(31) Stipa, P.; Greci, L.; Carloni, P.; Damiani, E. *Polym. Degrad. Stab.* **1997**, *55*, 323.